Macromolecules

ARTICLE

pubs.acs.org/Macromolecules

Novel Hyperbranched Ferrocene-Containing Poly(boro)carbosilanes Synthesized via a Convenient "$A_2 + B_3$" Approach

Jie Kong,[†,‡] Thomas Schmalz,[§] Günter Motz,[§] and Axel H. E. Müller*[,‡]

[†]Department of Applied Chemistry, School of Science, Northwestern Polytechnical University, Xi'an 710072, P. R. China

[‡]Macromolecular Chemistry II, University of Bayreuth, D-95440 Bayreuth, Germany

[§]Ceramic Materials Engineering, University of Bayreuth, D-95440 Bayreuth, Germany

Supporting Information

ABSTRACT: We report the synthesis of versatile hyperbranched ferrocene-containing poly(boro)carbosilanes (hb-PBCS) via a convenient "$A_2 + B_3$" approach. Two types of hb-PBCS are obtained by the hydrosilylation of 1,1′-bis-(dimethylsilyl)ferrocene (A_2) with trivinylmethylsilane (B_3) followed by modification with 9-borabicyclo[3.3.1]nonane (9-BBN) and by the hydroboration of 1,1′-bis(dimethyl-vinylsilyl)ferrocene (A_2) with the borane−dimethyl sulfide complex (B_3), respectively. Size exclusion chromatography (SEC) results demonstrate that the well-soluble hb-PBCS possess appreciable weight-average molecular weight ($M_{w,SEC}$) up to 62 300 g/mol with the polydispersity index (PDI) of 1.95−4.51. The combined characterization by $^{1}H-^{29}Si$ heteronuclear multiple-bond correlation (HMBC), ^{11}B nuclear magnetic resonance (NMR), and triple-detection SEC (triple-SEC) confirms the remarkable hyperbranched architecture of hb-PBCS with degrees of branching (DB) between 0.47 and 0.79. The Mark−Houwink−Sakurada exponents of hb-PBCS obtained from triple-SEC are significantly lower (α = 0.36−0.47) than that of their linear analogue (α = 0.69).

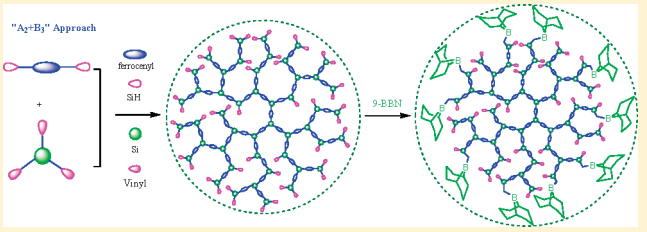

INTRODUCTION

The controlled pyrolysis of organometallic polymers has been proven to be a promising chemical approach to prepare advanced functional precursor-derived ceramics (PDCs) with diverse shapes such as fibers,[1] highly porous components,[2] and micro/nanoelectromechanical systems (M/NEMS).[3] Numerous organometallic polymers including poly(organosilylcarbodiimides),[4] polysiloxanes,[5] polysilazanes,[6] polyborosilazanes,[7] and metal-containing polymers[8] provided a large palette for manipulating the structures and properties of PDCs. Polyferrocenylsilanes (PFS) belong to a novel class of transition-metal-containing polymers that consist of alternating ferrocene and organosilane units on backbone. Since the preparation of high-molecular-weight PFS using thermal ring-opening polymerization was pioneered by Manners et al.,[9] PFS with linear, cyclic, or hyperbranched architecture and their block copolymers have shown potential in the formation of shaped magnetic ceramics[10,11] and the self-assembly into well-defined hybrid architectures such as micelle architectures,[12] spheres,[13] cylinders,[14] and one-dimensional nanostructures.[15]

Normally, PFS-derived ceramics possess tunable magnetic properties between the ferromagnetic and the superparamagnetic state by controlling the pyrolysis conditions of PFS.[10a] The incorporation of boron (even lower than 1 wt %) into silicon carbide and silicon nitride multiphase ceramics (SiCN) can significantly reduce their crystallinity at high temperature and improve thermal stabilities in air due to the oxidation resistance of the formed boron carbide (BC_4) and boron nitride (BN) phases.[16,17] When boron is incorporated into PFS to form ferrocenylboranes[18] and ferrocenylborane polymers,[19] multifunctional ceramics with tailorable magnetic properties and high-temperature resistance can be achieved under suitable pyrolysis conditions. Thus, the design and synthesis of boron-containing polyferrocenylsilanes are of great interest and importance for preparing advanced functional ceramics.[20]

Several synthetic approaches can be employed to introduce boron into organometallic polymers. Generally, they can be categorized into (i) direct polymerization of boron-containing monomers possessing a Si−Cl, B−Cl, B−Br, or B−H bond,[21] (ii) dehydrogenative coupling reaction of organometallic polymers with borane derivatives,[22] and (iii) hydroboration of unsaturated groups of organometallic polymers with monofunctional or multifunctional boranes.[23] These boranes are mainly 9-borabicyclo[3.3.1]nonane (9-BBN), pinacolborane, borazine, and the borane−dimethyl sulfide complex ($BH_3 \cdot SMe_2$). However, the direct polymerization of monomers with the B−Cl bond and the hydroboration of multifunctional borane such as $BH_3 \cdot SMe_2$ and borazine easily yields extensively cross-linked systems with poor processability.[24] As ceramic precursors, besides the versatile functionality, their favorable processing

Received: December 20, 2010
Revised: January 25, 2011
Published: February 14, 2011

Scheme 1. "$A_2 + B_3$" Combined Hydroboration Route To Synthesize Hyperbranched Ferrocene-Containing Poly(boro)carbosilanes with Boron Atoms on the Termini (hb-PBCS-BBN) (Approach 1)

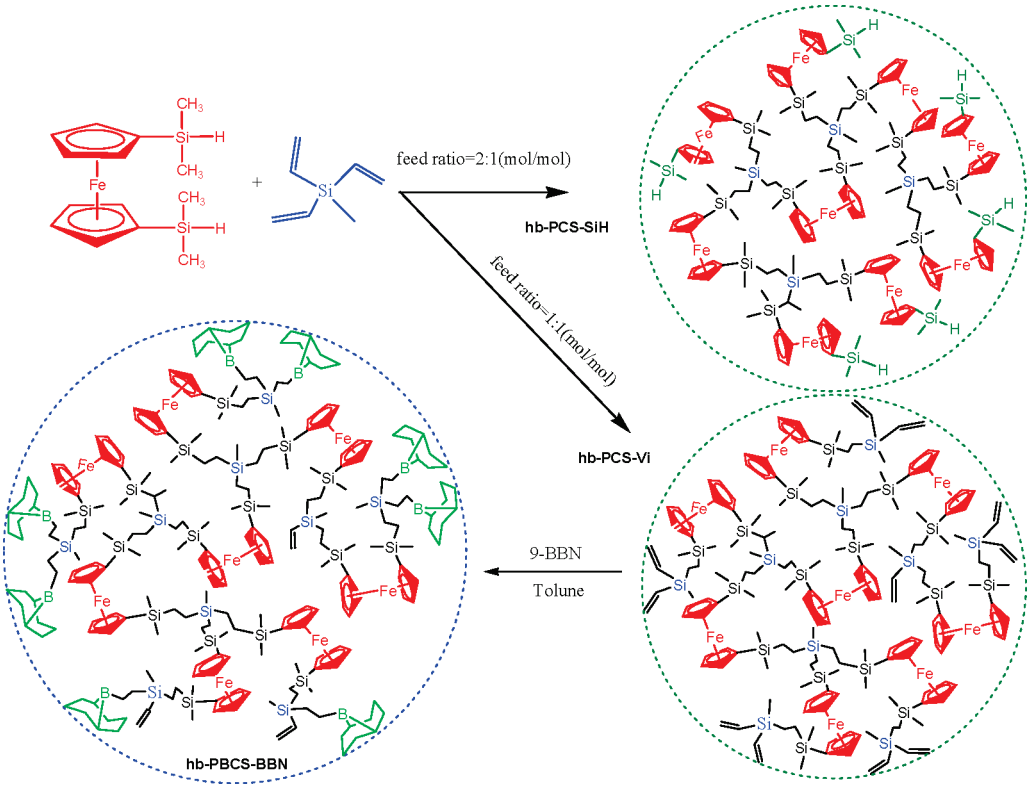

properties are also important especially for the formation of PDCs with the mentioned complex shapes.

Therefore, we propose the design and synthesis of a new type of boron-containing PFS, i.e., hyperbranched ferrocene-containing poly(boro)carbosilanes (hb-PBCS). The hyperbranched architecture, from our viewpoint, offers the following advantages: (i) For either monofunctional borane or multifunctional borane, boron can be conveniently introduced into the side groups or backbones of hb-PBCS by the hydroboration or the so-called "$A_2 + B_3$" approach based on boron-containing monomers.[25] (ii) hb-PBCS may possess higher solubility and lower viscosity compared to their linear counterparts due to the compact shape and decreased interchain entanglements.[26] Higher solubility and lower viscosity are especially favorable for preparing PDC by precursor infiltration and pyrolysis method. (iii) The hyperbranched architecture and compact conformation of hb-PBCS may be superior to retaining iron and boron distributed along the backbone or side groups that give a possibility to form magnetic and high-temperature resistant ceramic nanocrystals via a direct bulk pyrolysis.

Herein, we report the synthesis of versatile hb-PBCS via a convenient "$A_2 + B_3$" approach for the first time. First, hyperbranched ferrocene-containing polycarbosilanes (hb-PCSs) with vinyl terminals (hb-PCS-Vi) were prepared via the hydrosilylation of A_2 monomer, 1,1′-bis(dimethylsilyl)ferrocene, and B_3 monomer, trivinylmethylsilane. Then, hb-PBCS with boron atoms on the termini (hb-PBCS-BBN) were obtained by the hydroboration of hb-PCS-Vi-precursor and 9-BBN. This synthetic route is named approach 1 and is shown in Scheme 1. Alternatively, according to approach 2 presented in Scheme 2, i.e., direct "$A_2 + B_3$" synthetic route, hb-PBCS with boron atoms on the backbone (hb-PBCS-Vi) were generated directly by the hydroboration of A_2 monomer, 1,1′-bis(dimethylvinylsilyl)ferrocene, and B_3 monomer, $BH_3 \cdot SMe_2$. Afterward, their hyperbranched architectures were characterized by nuclear magnetic resonance (NMR) and triple-detection size exclusion chromatography (triple-SEC). Specifically, the conformation of the hyperbranched polymer was characterized via tapping-mode atomic force microscopy (AFM) and transmission electron microscopy (TEM).

EXPERIMENTAL SECTION

Materials. Ferrocene (98%), chlorodimethylsilane (98%), chlorodimethylvinylsilane (97%), *n*-butyllithium (1.6 M in hexane), *N,N,N′,N′*-tetramethylethylenediamine (TMEDA), borane−dimethyl sulfide complex (2 M in tetrahydrofuran), 9-borabicyclo[3.3.1]nonane (0.5 M in tetrahydrofuran), anhydrous acetonitrile, and diethyl ether were purchased from Sigma-Aldrich Co. Trivinylmethylsilane (95%), platinum−1,3-divinyl-1,1,3,3-tetramethyldisiloxane complex (0.1 M in polydimethylsiloxane terminated with vinyl) (Karstedt's catalyst), and platinum (5%, on carbon) catalyst (Pt/C) were received from ABCR GmbH & Co. KG. All the reagents were used as received without further treatment. Anhydrous hexane, toluene, and tetrahydrofuran (THF) were freshly distilled for use under reflux using sodium/benzophenone.

Synthesis of 1,1′-Bis(dimethylsilyl)ferrocene (1). Under an argon atmosphere, a 500 mL flame-dried flask equipped with a Teflon stir bar, septum, and high-vacuum stopcock was charged with ferrocene (5.58 g, 30 mmol), TMEDA (11 mL, 74 mmol), and anhydrous hexane (100 mL) at room temperature. Then *n*-butyllithium solution (29.6 mL, 74 mmol) was added through an argon-purged syringe. The reaction

dx.doi.org/10.1021/ma1029086 |*Macromolecules* 2011, 44, 1280–1291

Scheme 2. "$A_2 + B_3$" Route To Synthesize Hyperbranched Ferrocene-Containing Poly(boro)carbosilanes with Boron Atoms on the Backbone (hb-PBCS-Vi) (Approach 2)

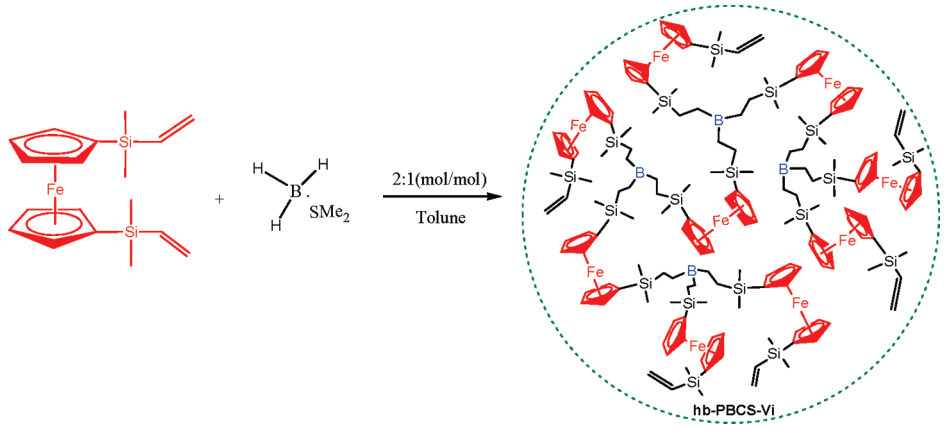

Table 1. Main Polymerization Results of Hyperbranched Ferrocene-Containing Polycarbosilanes (hb-PCS)

sample name	monomer	method[a]	$10^{-3}M_{w,SEC}$[b]	PDI[b]	$10^{-3}M_{w,triple}$[c]	PDI[c]	content of FG[d] (%)	DB[e]	DB[f]
hb-PCS-Vi1	**1**	I	62.3	4.33	282.0	4.13	3.5	0.77	0.71
hb-PCS-Vi2	**1**	II	27.6	3.32	41.3	3.13	5.5	0.61	0.54
hb-PCS-Vi3	**1**[g]	II	11.0	2.27			6.8	0.56	0.47
hb-PCS-Vi4	**1**[g]	III	6.1	1.95			5.8	0.50	0.47
hb-PCS-SiH1	**1**	I	49.5	4.51	152.1	5.17	1.3		0.79
hb-PCS-SiH2	**1**	II	29.9	3.78			1.2		
L-PFCS	**1**, **2**	I	5.4	1.48	5.9	1.26			

[a] I: the feed mole ratio of A_2 and B_3 was 1/1, and polymerization was conducted with three-batch adding of A_2. II: the feed mole ratio of A_2 and B_3 was 1/1, and polymerization was conducted with one-batch adding of A_2. III: using Pt/C as catalyst. [b] Both the molecular weight ($M_{w,SEC}$) and the polydispersity index (PDI) were determined by SEC with PS calibration. [c] Both the molecular weight ($M_{w,triple}$) and the polydispersity index (PDI) were determined by triple SEC. [d] The weight content of functional groups (FG), i.e., vinyl and Si−H, was estimated using ^{1}H NMR. [e] DB_{Frey} was determined by ^{29}Si NMR. [f] $DB_{Fréchet}$ was determined by ^{29}Si NMR. [g] Monomer **1** contains monosubstituted monomer A_1.

mixture was stirred for 6 h at room temperature and became slurry. In a glovebox, the slurry was added into another 500 mL flame-dried flask at −78 °C (dry ice/acetone bath) that had been charged with chlorodimethylsilane (17.40 g, 180 mmol) and anhydrous hexane. The mixture was heated to room temperature again and stirred overnight. Upon completion of the reaction, the solvent and excess reagents were removed under vacuum line. After the filtration and rotary evaporation (20 mbar, 50 °C), the crude product was purified by column chromatography (silica gel size 70−100 μm, column diameter 7 cm, column length 30 cm) using hexane as elute, yielding 1,1′-bis(dimethylsilyl)-ferrocene (**1**) as brown liquid (4.8 g, 48.3% yield). ^{1}H NMR (**1**, $CDCl_3$, ppm): 0.35−0.40 (12H, $Si(CH_3)_2-H$), 4.42−4.51 (2H, $Si(CH_3)_2-H$), 4.13−4.18 (4H, η^5-C_5H_4), 4.33−4.38 (4H, η^5-C_5H_4). ^{13}C NMR (**1**, $CDCl_3$, ppm): −2.94 (4C, $Si(CH_3)_2-H$), 68.30 (2C, η^5-C_5H_4), 71.65 (4C, η^5-C_5H_4), 73.75 (4C, η^5-C_5H_4). ^{29}Si NMR (**1**, $CDCl_3$, ppm): −18.62 (2Si, $-(CH_3)_2Si-H$). FT-IR (**1**, KBr, cm^{-1}): 2110 (ν Si−H), 1247 (ν Si−CH_3), 1442 (ν η^5-C_5H_4). Mass spectrum (MS): m/z: calcd (%) for $C_{14}H_{22}FeSi_2$: 302; found: 302. Elemental analysis: calcd (%) for $C_{14}H_{22}FeSi_2$: C 55.63, H 7.28; found: C 55.59, H 7.15.

Synthesis of 1,1′-Bis(dimethylvinylsilyl)ferrocene (2). The synthesis procedure of **2** was similar to **1**, but with chlorodimethylvinylsilane (22.4 g, 180 mmol) instead of chlorodimethylsilane. The product of **2** is also a brown liquid (3.3 g, 31.1% yield). ^{1}H NMR ($CDCl_3$, ppm): 0.36−0.38 (12H, $-Si(CH_3)_2-$), 4.10−4.13 (4H, η^5-C_5H_4), 4.36−4.39 (4H, η^5-C_5H_4). 5.72−5.80 (2H, Si−CH=CH_2), 6.00−6.06 (2H, Si−CH=CH_2), 6.25−6.40 (2H, Si−CH=CH_2). ^{13}C NMR ($CDCl_3$, ppm): −2.24−1.51 (4C, $Si(CH_3)_2$), 70.05 (2C, η^5-C_5H_4), 71.50 (4C, η^5-C_5H_4), 73.20 (4C, η^5-C_5H_4), 131.77 (2C, Si−CH=CH_2), 139.14 (2C, Si−CH=CH_2). ^{29}Si NMR ($CDCl_3$, ppm): −10.32 (2Si, $-Si(CH_3)_2-CH=CH_2$). FT-IR (KBr, cm^{-1}): 1403, 1593 (ν −CH=CH_2), 1247 (ν Si−CH_3), 1422 (ν η^5-C_5H_4). MS: m/z: calcd (%) for $C_{18}H_{26}FeSi_2$: 354; found: 354. Elemental analysis: calcd (%) for $C_{18}H_{26}FeSi_2$: C 61.02, H 7.40; found: C 61.51, H 7.27.

Preparation of hb-PCS with Vinyl Terminals (hb-PCS-Vi). Under an argon atmosphere, a flame-dried flask equipped with a Teflon stir bar, septum, and high-vacuum stopcock was charged with trivinylmethylsilane (TVMS, 0.37 g, 3.0 mmol), 6.5 mg of Karstedt's catalyst, and 15.0 mL of toluene. At 45 °C, monomer **1** (0.91 g, 3.0 mmol) was added into the solution by one-batch addition or three-batch addition with interval of 30 min. The reaction mixture was stirred 8−12 h at 45 °C and monitored by FTIR spectroscopy until Si−H bond resonance at 2110 cm^{-1} disappeared. Then the solvent was removed by rotary evaporation (40 mbar, 50 °C) yielding brown elastomers. The crude product was soluble in 5 mL of diethyl ether and precipitated into 50 mL of methanol for three times. Then the precipitate was dried in vacuum oven for 2 days (10 mbar, 60 °C). The hb-PCS-Vi were obtained as brown elastomers (70−81% yield). Specific reaction conditions are summarized in Table 1. ^{1}H NMR ($CDCl_3$, ppm): −0.08−0.00 ($SiCH_3$), 0.06 (=$SiCH_3$−CH=CH_2), 0.11 ($-SiCH_3(CH=CH_2)_2$), 0.18−0.40 ($-Si(CH_3)_2-$), 0.41−0.62 (Si−CH_2-CH_2−Si), 0.91 (Si−CH-(CH_3)−Si), 1.29 (Si−CH(CH_3)−Si), 4.01−4.28 (η-C_5H_4), 5.62−5.78 (Si−CH=CH_2), 5.96−6.07 (Si−CH=CH_2), 6.11−6.24

Table 2. Main Polymerization Results of Hyperbranched Ferrocene-Containing Polyborocarbosilanes (hb-PBCS)

sample name	approach	precursor	feed ratio of 9-BBN to precursor	$10^{-3}M_{w,SEC}$[a]	PDI[a]	content of FG[b] (%)
hb-PBCS-BBN1	1	HB-PFCS-Vi2	1:12	55.7	5.43	5.5
hb-PBCS-BBN2	1	HB-PFCS-Vi2	1:30	38.5	4.11	2.0
hb-PBCS-BBN3	1	HB-PFCS-Vi4	1:12	7.9	2.13	5.5
hb-PBCS-BBN4	1	HB-PFCS-Vi4	1:30	7.3	2.11	4.5
hb-PBCS-Vi1	2			5.8[c]	1.65[c]	4.5
hb-PBCS-Vi2	2			3.5[c]	1.41[c]	4.8

[a] Both the molecular weight ($M_{w,SEC}$) and the polydispersity index (PDI) were determined by SEC with PS calibration. [b] The weight content of functional groups (FG), i.e., 9-BBN and vinyl, were estimated using ^{1}H NMR. [c] The molecular weight and PDI were determined by triple-SEC.

(Si−CH=CH_2). ^{13}C NMR ($CDCl_3$, ppm): −6.4 ($SiCH_3$−CH=CH_2), −2.8 ($SiCH_3(CH=CH_2)_2$), 1.0 (−$Si(CH_3)_2$−), 4.7, 8.9 (Si-CH_2−CH_2−Si), −1.7 (Si−$CH(CH_3)$−Si), 8.3 (Si−$CH(CH_3)$−Si), 71, 73 (η^5-C_5H_4), 132.2 (Si−CH=CH_2), 137.8 (Si−CH=CH_2). ^{29}Si NMR ($CDCl_3$, ppm): 7.98 (dendritic unit), −0.6 (backbone), −1.41 (linear unit), −11.16 (terminal unit). FT-IR (KBr, cm^{-1}): 1403, 1593 (ν −CH=CH_2), 1247 (ν Si−CH_3), 1422 (ν η-C_5H_4). Representative molecular weight: $M_{w,SEC}$ = 62 300, M_w/M_n = 4.33 (hb-PCS-Vi1).

Synthesis of hb-PCS with Si−H Terminals (hb-PCS-SiH). The synthesis procedure of hb-PCS with SiH terminals (hb-PCS-SiH) was similar to hb-PCS-Vi, but with 6.0 mmol of **1** (1.82 g,) instead of 3.0 mmol. The hb-PCS-SiH were obtained as brown elastomers (74−82% yield). ^{1}H NMR ($CDCl_3$, ppm): −0.05−0.00 ($SiCH_3$), 0.10−0.13 ((η^5-C_5H_4)−$Si(CH_3)_2$−H), 0.18−0.38 ((η^5-C_5H_4)−$Si(CH_3)_2$−(η^5-C_5H_4)), 0.40−0.62 (Si−CH_2−CH_2−Si), 0.88−0.93 (Si−$CH(CH_3)$−Si), 1.27 (Si−CH (CH_3)−Si), 4.00−4.18 (η-C_5H_4), 4.20−4.38 (η-C_5H_4), 4.65−4.75 (Si−H). ^{13}C NMR ($CDCl_3$, ppm): −6.8 ($SiCH_3$), −3.1 ((η^5-C_5H_4)−$Si(CH_3)_2$−(η^5-C_5H_4)), 1.87 ((η^5-C_5H_4)−$Si(CH_3)_2$−H), 5.83 (Si−CH_2−CH_2−Si), 10.21 (Si−CH_2−CH_2−Si), 72.1, 72.2, 74.2 (η^5-C_5H_4). ^{29}Si NMR ($CDCl_3$, ppm): 8.0 (dendritic unit), −0.7 (backbone), −18.5 (linear or terminal unit). FT-IR (KBr, cm^{-1}): 2110 (ν Si−H), 1247 (ν Si−CH_3), 1442 (ν η^5-C_5H_4). Representative molecular weight: $M_{w,SEC}$ = 49 500, M_w/M_n = 4.51 (hb-PCS-SiH1).

Preparation of hb-PBCS-BBN via Approach 1. Under an argon atmosphere, a flame-dried tube equipped with a Teflon stir bar, septum, and high-vacuum stopcock was charged with 300 mg of hb-PCS-Vi and 5 mL of anhydrous THF. After evacuating the tube for 30 min to degas, 9-BBN (0.5 M in THF) was dropped using an argon-purged syringe. Specific reaction conditions are listed in Table 2. After the completion, the solvent was removed under vacuum line coupled with trap bottle surrounded with liquid nitrogen, yielding brown solids (hb-PBCS-BBN) (94−98% yield). ^{1}H NMR ($CDCl_3$, ppm): −0.08−0.00 ($SiCH_3$), 0.06 ($SiCH_3$−CH=CH_2), 0.11 (−$SiCH_3(CH=CH_2)_2$), 0.18−0.40 (−$Si(CH_3)_2$−), 0.41−0.62 (Si−CH_2−CH_2−Si), 0.91 (Si−$CH(CH_3)$−Si), 1.29 (Si−$CH(CH_3)$−Si), 4.01−4.28 (η^5-C_5H_4), 0.96 (Si−CH_2−CH_2−B), 1.24 (Si−CH_2−CH_2−B), 1.35−1.81 (proton on 9-BBN), 4.14, 4.33 (η^5-C_5H_4), 5.62−5.78 (Si−CH=CH_2), 5.96−6.07 (Si−CH=CH_2), 6.11−6.24 (Si−CH=CH_2). ^{13}C NMR ($CDCl_3$, ppm): −6.4 (=(CH_3)Si−CH=CH_2), −2.8 (−(CH_3)Si−$(CH=CH_2)_2$), 1.0 (−$(CH_3)_2$Si−), 4.7 (Si−CH_2−CH_2−Si), 8.9 (Si−CH_2−CH_2−Si), −1.7 (Si−$CH(CH_3)$−Si), 8.3 Si−$CH(CH_3)$−Si), 71, 73 (η^5-C_5H_4), 132.2 (Si−CH=CH_2), 137.8 (Si−CH=CH_2), 22.4, 27.2, 32.6. 41.9 (9-BBN). FT-IR (KBr, cm^{-1}): 1403, 1593 (ν −CH=CH_2), 1247 (ν Si−CH_3), 1422 (ν η^5-C_5H_4). Representative molecular weight: $M_{w,SEC}$ = 55 700, M_w/M_n = 5.43 (hb-PBCS-BBN1).

Synthesis of hb-PBCS-Vi via Approach 2. Under an argon atmosphere, a flame-dried tube equipped with a Teflon stir bar, septum, and high-vacuum stopcock was charged with monomer **2** (0.71 g, 2.0 mmol) and 15.0 mL of anhydrous THF. After evacuating the tube for 30 min to degas, 1 mL of BH_3·SMe_2 solution (2 M in THF) was dropped using an argon-purged syringe. The reaction mixture was stirred 8−12 h at 25 °C. Upon completion of the reaction, the solvent and dimethyl sulfide were removed under vacuum at 60 °C, thus yielding yellow solids (hb-PBCS-Vi) (95−96% yield). ^{1}H NMR ($CDCl_3$, ppm): 0.22−0.43 (−$Si(CH_3)_2$−), 1.11 (Si−CH_2−CH_2−B), 0.90 (Si−CH_2−CH_2−B), 4.01−4.12, 4.16−4.37 (η^5-C_5H_4), 5.62−5.78 (Si−CH=CH_2), 5.96−6.07 (Si−CH=CH_2), 6.11−6.24 (Si−CH=CH_2). ^{13}C NMR ($CDCl_3$, ppm): −2.7 (−$Si(CH_3)_2$−), 10.33 (Si−CH_2−CH_2−B), 25.41 (Si−CH_2−CH_2−B), 71.1, 71.2, 73.3 (η^5-C_5H_4), 131.8 (Si−CH=CH_2), 138.9 (Si−CH=CH_2). Representative molecular weight: $M_{w,triple}$ = 5800, M_w/M_n = 1.65 (hb-PBCS-Vis1).

Preparation of Linear Poly(ferrocenyl)carbosilane (L-PCS). Under an insert argon atmosphere, a dried flask was charged with monomer **1** (0.30 g, 1.0 mmol), 3.0 mg of Karstedt's catalyst, and 15.0 mL of anhydrous toluene. At 40 °C, monomer **2** (0.35 g, 1.0 mmol) was added into the solution using an argon-purged syringe. The reaction mixture was stirred 12 h at 40 °C and monitored by FTIR spectroscopy until the Si−H bond resonance at 2110 cm^{-1} disappeared. The crude product was precipitated using diethyl ether and dried in vacuum oven for 2 days (10 mbar, 60 °C), yielding L-PCS as yellow solids (82% yield). ^{1}H NMR ($CDCl_3$, ppm): 0.24 ((η^5-C_5H_4)−Si−$(CH_3)_2$−(η^5-C_5H_4)), 0.58 (Si−CH_2−CH_2−Si), 0.91 (Si−$CH(CH_3)$−Si), 1.29 (Si−$CH(CH_3)$−Si), 4.01−4.28 (η^5-C_5H_4). FT-IR (KBr, cm^{-1}): 1247 (ν Si−CH_3), 1422 (ν η^5-C_5H_4). Representative molecular weight: $M_{w,SEC}$ = 5400, M_w/M_n = 1.48 (L-PCS).

Characterization. *Nuclear magnetic resonance (NMR)* measurements were carried out on a Bruker AC-250 spectrometer (Bruker BioSpin, Switzerland) to collect the ^{1}H and ^{13}C spectra. ^{29}Si NMR spectra were recorded on a Bruker Avance 500 spectrometer (Bruker BioSpin, Switzerland) operating at 50.7 MHz in $CDCl_3$ or C_6D_6. Chemical shifts are referenced to tetramethylsilane (TMS). Long-range ^{1}H−^{29}Si heteronuclear multiple-bond correlation (^{1}H−^{29}Si HMBC) spectra were acquired with pulse field gradients in absolute value mode. The multiple-bond delay was adjusted to a coupling constant of 5 Hz. The data were collected in an 8192 × 256 matrix with 8 transients per t_1 increment. The recycle period was 1.5 s. Sine-bell window functions were applied before Fourier transformation in a 2048 × 1024 matrix. ^{11}B NMR spectra were obtained on a Varian Inova 400 MHz spectrometer (Varian Inc.) equipped with the appropriate decoupling accessories. The ^{11}B chemical shifts are referenced to BF_3·OEt_2 (0.0 ppm) with a negative sign indicating an upfield shift.

Fourier transform infrared spectroscopy (FT-IR) measurements were conducted on a FT-IR spectrophotometer (Perkin-Elmer).

Elemental analyses were performed on a Vario Elementar EL III (Elementar Analysensysteme GmbH, Germany).

Mass spectra (MS) were recorded using a Varian Mat 311 A (Varian Inc.).

Size exclusion chromatography (SEC) measurements were performed at room temperature on an apparatus equipped with four PSS−SDV gel columns (5 μm) with a porosity range from 10^2 to 10^5 Å (PSS, Mainz, Germany) and together with a differential refractometer and an ultraviolet detector at 254 nm. THF (1% toluene as an internal standard) was used as an eluent with a flow rate of 1.0 mL/min. Polystyrene (PS)

Scheme 3. Synthetic Route of 1,1′-Bis(dimethylsilyl)-ferrocene (1) and 1,1′-Bis(dimethylvinylsilyl)ferrocene (2)

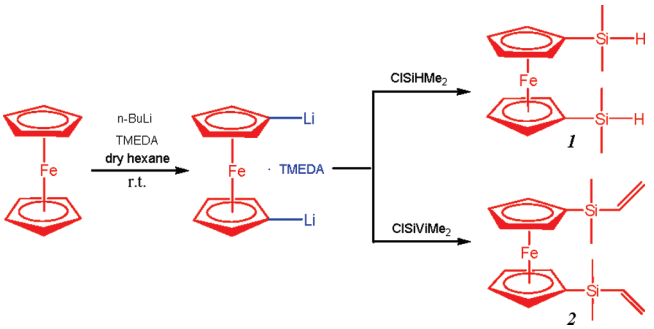

standards with narrow molecular weight distribution (PSS, Mainz) were used for the calibration.

Triple-detection size exclusion chromatography (triple-SEC) measurements were conducted on an Agilent HPLC system equipped with three PSS−SDV gel columns (10^6 Å, 5 μm; 10^5 Å, 5 μm; 10^3 Å, 5 μm) with a flow rate of 0.8 mL/min in THF (HPLC grade) at room temperature. Detectors were including differential refractometer (Agilent Technologies 1200), multiangle light scattering detector (MALS) equipped with a 632.8 nm He−Ne laser (DAWN HELEOS, Wyatt), and viscometer (ViscoStar II, Wyatt). The MALS detector was used to determine the molecular weight, whereas the viscometer provided Mark−Houwink−Sakurada relationships. The refractive index increments of polymers in THF were measured at 25 °C using a PSS DnDc-2010/620 differential refractometer.

RESULTS AND DISCUSSION

Synthesis of A_2 Monomers. For the synthesis of hb-PBCS via either approach 1 or approach 2, the purity of monomers is a key factor to controlling molecular weights and hyperbranched architectures. Since the B_3 monomers, trivinylmethylsilane and $BH_3 \cdot SMe_2$, are commercial products, the highly pure A_2 monomers, 1,1′-bis(dimethylsilyl)ferrocene (**1**) and 1,1′-bis(dimethylvinylsilyl)ferrocene (**2**), are of great importance. As shown in Scheme 3, A_2 monomers were synthesized via coupling reaction of dilithioferrocene with chlorodimethylsilane and chlorodimethylvinylsilane, respectively.[27,28] An excess of *n*-butyllithium and chlorosilane to ferrocene and a subsequent column chromatography fractionation using silica gel were employed to obtain A_2 monomers with high purity.

Figure 1a shows the ^{1}H NMR spectrum of monomer **1** in $CDCl_3$. The signals at 4.15 and 4.35 ppm corresponded to the protons on cyclopentadienyl (Cp) rings after symmetric substitution of double dimethlysilyl groups. The dimethlysilyl group can also be verified from the obvious heptuplet peak in the region of 4.42−4.51 ppm. So the clear assignment and matched integral values of all protons indicate the successful synthesis of monomer **1**. ^{13}C NMR (Figure 1b) and ^{29}Si NMR (Figure S1, Supporting Information) further confirm its molecular structure, where all the carbon atoms and silicon atoms are clearly assigned. Additional evidence comes from MS (Figure S2) where the single peak at 302 is in good agreement with the theoretical mass-to-charge ratio of monomer **1**. In contrast, A_2 monomer containing monosubstituted dimethylvinylsilylferrocene (A_1) was prepared. Its ^{1}H NMR spectrum (Figure S3) shows complex signals, where five main peaks appear in the region of 4.1−4.4 ppm. Specifically, the sharp signal at 4.17 ppm corresponded to the

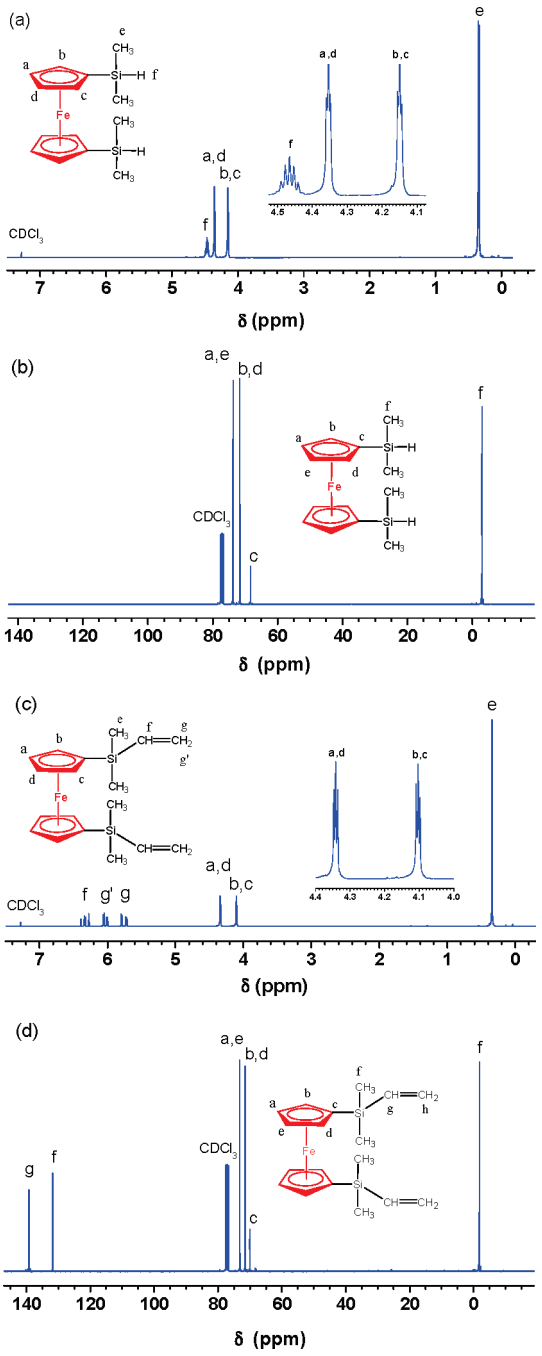

Figure 1. NMR spectra of 1,1′-bis(dimethylsilyl)ferrocene (**1**) and 1,1′-bis(dimethylvinylsilyl)ferrocene (**2**) in $CDCl_3$: (a) ^{1}H NMR of **1**, (b) ^{13}C NMR of **1**, (c) ^{1}H NMR of **2**, (d) ^{13}C NMR of **2**.

protons of Cp ring without substitution in A_1. The content of A_1 can be calculated from the integral area ratio on ^{1}H NMR, which is important to control molecular weight of hb-PCS as described later.

The ^{1}H NMR spectrum of monomer **2** in $CDCl_3$ is presented in Figure 1c. Similar to monomer **1**, the signals at 4.15 and 4.35 ppm corresponded to the protons on Cp rings after symmetric substitution of double dimethylvinylsilyl groups. The dimethylvinylsilyl group was verified from the obvious three signal peaks in the region of 5.7−6.4 ppm. Moreover, the integral areas of all the protons matched the theoretical value of monomer **2** indicated its

dx.doi.org/10.1021/ma1029086 |*Macromolecules* 2011, 44, 1280–1291

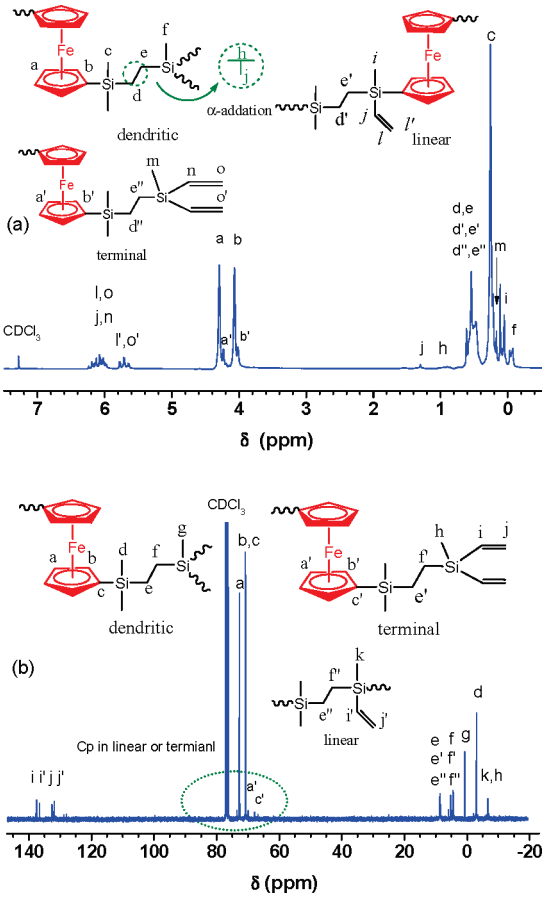

Figure 2. NMR spectra of a representative hb-PCS-Vi2 in $CDCl_3$: (a) ^1H NMR; (b) ^{13}C NMR.

high purity. Evidence coming from ^{13}C NMR (Figure 1d), ^{29}Si NMR (Figure S1), and MS (single peak at 354, Figure S2) also indicated the successful synthesis of monomer **2**.

Hyperbranched Ferrocene-Containing Polycarbosilanes (hb-PCS). As illustrated in Scheme 1, hb-PCS were prepared via the hydrosilylation of A_2 monomer, 1,1′-bis(dimethylsilyl)ferrocene, and B_3 monomer, trivinylmethylsilane (TVMS), by using Pt/C catalyst or Karstedt's catalyst. In this approach, the terminals of hb-PCS are tunable by regulating the feed ratio of monomers. The starting ratio monomer **1**/TVMS of 1:1 and 2:1 resulted in hb-PCS with vinyl terminals (hb-PCS-Vi) and hb-PCS with Si−H terminals (hb-PCS-SiH), respectively. The molecular weights obtained under specific reaction conditions are summarized in Table 1. The weight-average molecular weight ($M_{w,SEC}$) of hb-PCS is 6200−62 300 g/mol with the polydispersity index (PDI) of 1.95−4.51 calibrated by PS standards. Both hb-PCS-Vi and hb-PCS-SiH are in brown elastomer-like states and possess high solubility in aliphatic and aromatic solvents. They are stable to air and moisture, which gives conveniences for further characterizations.

Figure 2 shows the ^1H and ^{13}C NMR spectra of hb-PCS-Vi in $CDCl_3$. Compared to the starting monomer **1** (Figure 1a), the characteristic signals of proton on Si−H bond (4.42−4.51 ppm) totally disappeared. At the same time, the broad peaks in the region of 0.41−0.62 ppm arising from the protons of formed alkyl bridges appeared. On the other hand, the decreased integral area of vinyl protons at 5.6−6.2 ppm ($SiCH_3$ as an internal

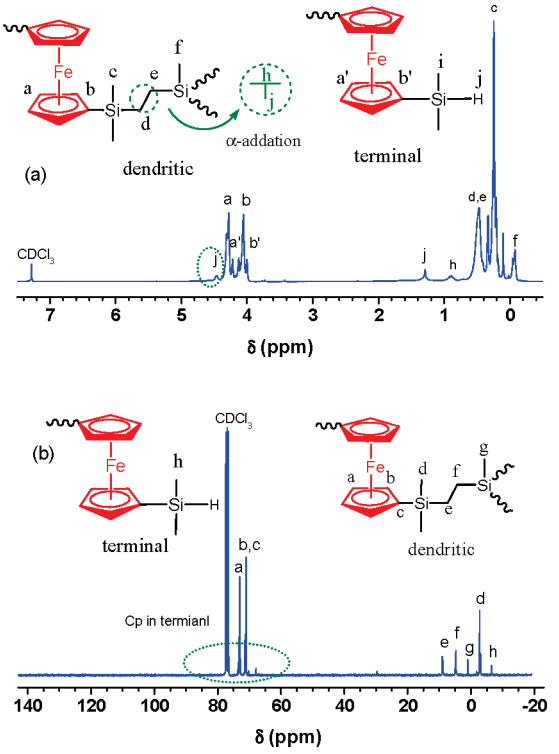

Figure 3. NMR spectra of a representative hb-PCS-SiH1 in $CDCl_3$: (a) ^1H NMR; (b) ^{13}C NMR.

standard) compared to the starting TVMS (Figure S4) reveals the hydrosilylation between monomer **1** and TVMS. Disappearance of Si−H bond and the reservation of vinyl groups suggest the vinyl end groups on hb-PCS-Vi. In addition, the ^{13}C NMR spectrum in Figure 2b identifies vinyl functional groups of hb-PCS-Vi, which signal peaks are in the region of 131.9−137.6 ppm. However, the clear identification of linear unit or terminal unit of hb-PCS-Vi proposed in Scheme 1 is dependent on the later ^{29}Si NMR analysis.

Different from hb-PCS-Vi, the ^1H NMR spectrum of hb-PCS-SiH in Figure 3a indicates that the characteristic signals of vinyl protons from TVMS (Figure S4) completely disappear, resulting in the broad signal peaks in the region of 0.40−0.63 ppm corresponding to the protons of alkyl bridges. The ^{13}C NMR spectrum in Figure 3b confirms the alkyl bridges. A small signal of proton on Si−H bond at 4.5 ppm is observed, which is also confirmed by its FT-IR resonance at 2110 cm^{-1} (Figure S5). As we expect, the NMR analysis demonstrates that hb-PCS with vinyl or Si−H terminals can be conveniently synthesized by regulating the feed ratio of monomers.

In addition, the strong ethylene signals in the region of 0.40−0.63 ppm show that β-addition dominates the hydrosilylation between monomer **1** and TVMS. In contrast, for either hb-PCS-Vi or hb-PCS-SiH, only two small signals in the region of 0.9−1.3 ppm can be found on ^1H NMR spectra. It indicates that only a few α-addition products are generated during the hydrosilylation. From the integral area ratio, the content of α-addition products is about 5% and 8% for hb-PCS-Vi and hb-PCS-SiH, respectively.

Degree of Branching of hb-PCS. As mentioned above, the identification of dendritic, linear, and terminal unit of hb-PCS depends on ^{29}Si NMR analysis. Herein, we employ $^1H-^{29}Si$

dx.doi.org/10.1021/ma1029086 |*Macromolecules* 2011, 44, 1280–1291

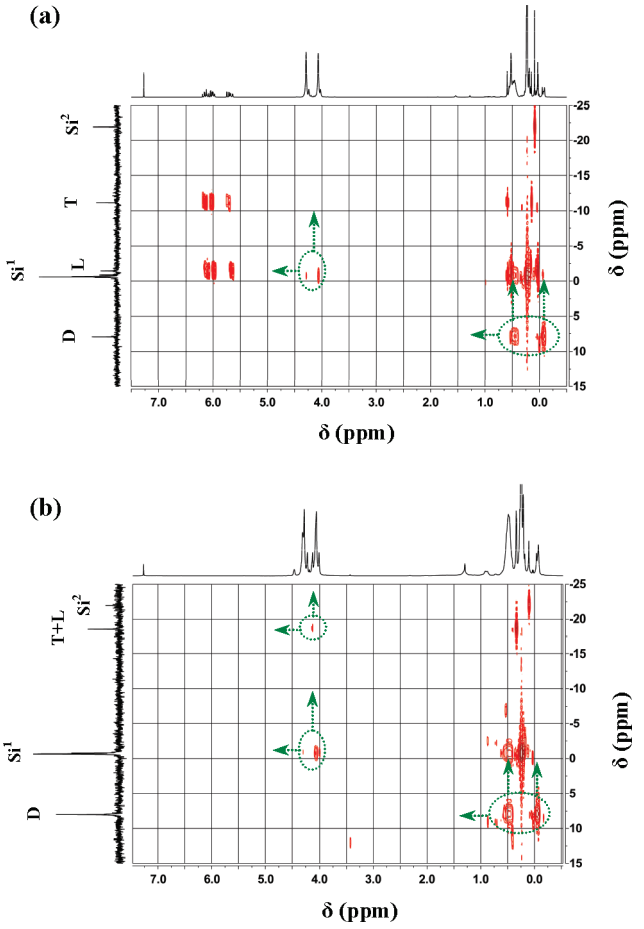

Figure 4. $^{1}H-^{29}Si$ HMBC NMR spectra of hb-PCS in $CDCl_3$: (a) hb-PCS-Vi2; (b) hb-PCS-SiH1.

HMBC to analyze hyperbranched architecture. Figure 4 shows the $^{1}H-^{29}Si$ HMBC spectra of hb-PCS-Vi and hb-PCS-SiH in $CDCl_3$. The possible chemical environments of silicon atoms in hb-PCS are illustrated in Chart 1. Here, silicon atom labeled D, L, and T represents dendritic, linear, and terminal unit, respectively. Si^1 and Si^2 represent the silicon atom linked on Cp ring and silicon atom from Karstedt's catalyst, respectively. They can be clearly identified from $^{1}H-^{29}Si$ HMBC according to the correlation of silicon atom and bonded groups such as vinyl, ethylene, silicon methyl, and Cp ring.

For hb-PCS-Vi, from Figure 4a, the signal at 7.98 ppm on ^{29}Si NMR is assigned to silicon atom that is correlated with silicon methyl (−0.2−0.05 ppm on ^{1}H NMR) and ethylene (0.4−0.6 ppm on ^{1}H NMR). Actually, it is defined as dendritic unit (D). Similarly, silicon atom linked on Cp ring (Si^1) shows the signal at −0.6 ppm on ^{29}Si NMR correlated with Cp rings (4.15, 4.35 ppm on ^{1}H NMR) and ethylenes (0.4−0.6 ppm on ^{1}H NMR). Moreover, the two signals at −1.41 and −11.16 ppm on ^{29}Si NMR correlated with silicon methyl (−0.2−0.05 ppm on ^{1}H NMR), ethylene (0.4−0.6 ppm on ^{1}H NMR), and vinyl (5.6−6.2 ppm on ^{1}H NMR). They are assigned to the linear unit (L) and terminal unit (T), respectively. For hb-PCS-SiH, there is only one signal at −18.5 ppm, corresponding to the silicon atom on linear unit (L) or terminal unit (T). The $^{1}H-^{29}Si$ HMBC analysis suggests their low content of L and T, which is in good agreement with the content of Si−H bond (1.2−1.3%) as shown in Table 1.

Chart 1. Possible Si Chemical Environments for hb-PCS

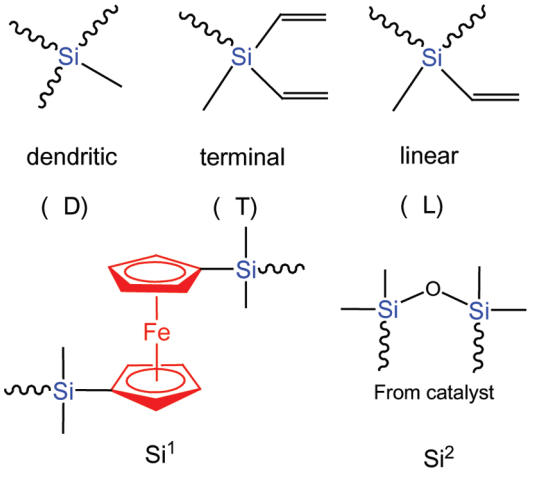

Microenvironments for silicon atoms in hb-PCS-Vi

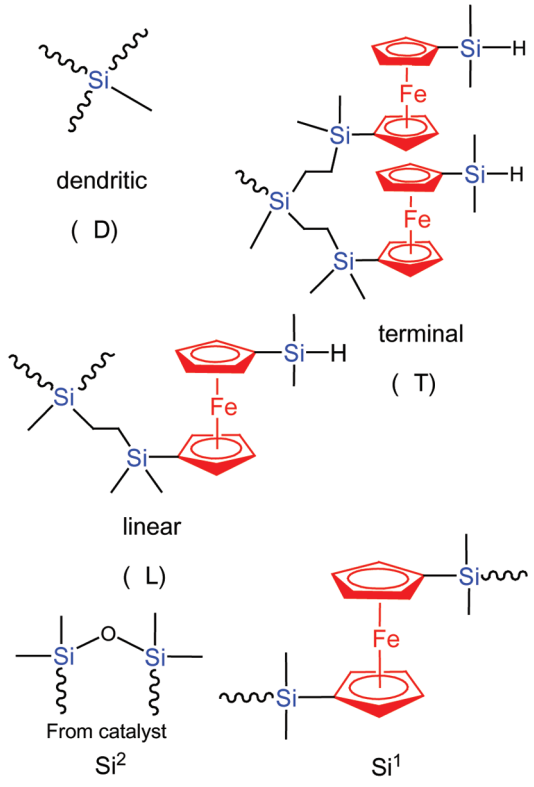

Microenvironments for silicon atoms in hb-PCS-SiH

According to Frey's and Fréchet's definition,[29,30] DB of hyperbranched polymer can be expressed as eqs 1 and 2, respectively

$$DB_{\text{Frey}} = \frac{2D}{2D+L} \quad (1)$$

$$DB_{\text{Frechet}} = \frac{D+T}{D+T+L} \quad (2)$$

where D, L, and T denote the mole fraction of dendritic, linear, and terminal units in hyperbranched polymer, respectively. From

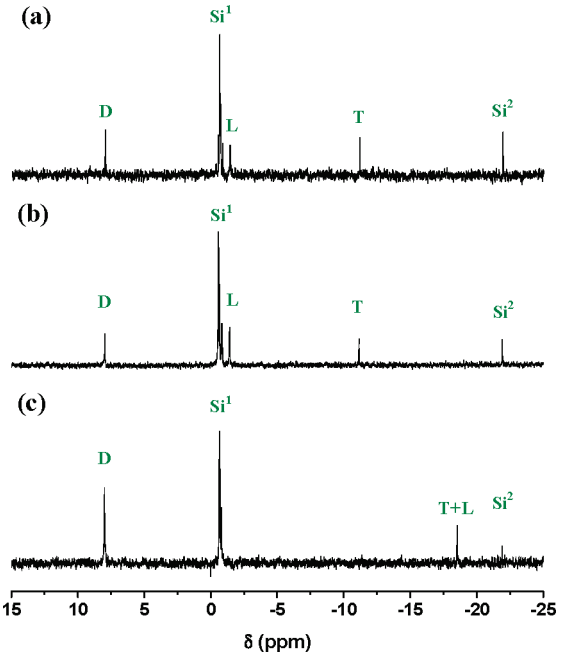

Figure 5. ^{29}Si NMR spectra of hb-PCS in $CDCl_3$: (a) hb-PCS-Vi2, (b) hb-PCS-Vi4, (c) hb-PCS-SiH1.

the NMR spectra, the mole fraction of D, L, and T can be calculated from the relative integration ratio. The ^{29}Si NMR spectra of hb-PCS are presented in Figure 5, and the according DB values are summarized in Table 1.

For hb-PCS-Vis, the DB_{Frey} and $DB_{Fréchet}$ are in the wide range of 0.47−0.77 according to different polymerization process summarized in Table 1. Compared to the DB around 0.50 of hyperbranched polymers synthesized with AB_2 monomers,[31] the high DB values of hb-PCS are due to the high "A" and "B" ratio (0.67−1.33) in the "$A_2 + B_3$" approach. For hb-PCS-SiH, there is almost no difference of silicon chemical environment between L and D unit on ^{29}Si NMR. So only the approximate $DB_{Fréchet}$ value of 0.79 was obtained. Similar to the results of theoretical kinetics of hyperbranched "$A_2 + B_3$" systems,[32] the DB is increased from 0.54 to 0.79 with increasing A:B ratio from 2:3 to 4:3. The reason is that the excess of "A" groups completely consumed the "B" groups, resulting in dendritic units rather than linear units. Therefore, the high DB value from ^{29}Si NMR suggests their regular hyperbranched architectures of hb-PCS via approach 1.

Molecular Weight Control of hb-PCS. Compared to the AB_g monomer strategy, the "$A_2 + B_3$" approach normally needs a strict control of the reaction conditions, such as time, concentration, addition rate, and sequence, to terminate reactions prior to cross-linking.[33] Here, because of the high steric hindrance of the ferrocenyl group of A_2 monomer, cross-linking can be avoided under the employed reaction conditions. In contrast, from our experience, if the 1,1′,4,4′-tetramethylsiloxane was used as A_2 monomer instead of monomer **1**, the cross-linking occurred rapidly even at room temperature. So here we mainly focused on the effect of addition mode and purity of A_2 monomer on the molecular weight. The SEC traces of hb-PCS-Vi are presented in Figure 6, and the according molecular weights are summarized in Table 1.

First, by regulating the polymerization process, hb-PCS-Vi1 with the highest $M_{w,SEC}$ of 62 300 g/mol and the PDI of 4.33 as measured by normal SEC can be obtained. Triple-SEC reveals much higher $M_{w,triple}$ = 282 000 g/mol with the PDI of 4.13 for the same hb-PCS-Vi1 sample. The multiangle light scattering detector avoids the mismatch between hyperbranched architecture and linear PS calibration in normal SEC.[34] Anyway, both SEC results indicate that hb-PCS with appreciable molecular weight can be prepared via approach 1.

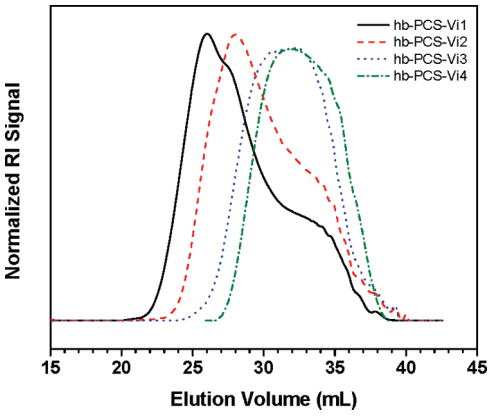

Figure 6. SEC traces (RI signal) of hb-PCS-Vi obtained from the normal SEC.

Second, the multibatch addition of monomer **1** into TVMS is helpful to increase the molecular weight of hb-PCS. It is seen by the higher molecular weights of hb-PCS-Vi1 and hb-PCS-SiH1 (three batch addition) than those of hb-PCS-Vi2 and hb-PCS-SiH2 (one batch addition). The increased molecular weight here is in accordance with the results of slow addition of AB_2 monomer in the work of Moore et al.[35] On the other hand, the DB value is also increased from 0.54 to 0.71 for hb-PCS-Vi. For the hyperbranched polymers via self-condensing vinyl polymerization (SCVP),[36] we also found that the DB of polymer obtained from multibatch addition was higher than that from one-batch addition.

Third, the molecular weight of hb-PCSs is drastically affected by the content of monosubstituted monomer A_1 in the A_2 monomer. In Figure 7, the molecular weight decreases with the increase of content of A_1 because A_1 terminates the growth of hyperbranched polymers. When the content of A_1 is higher than 15%, only products with low M_w can be obtained. Compared to dilithiumferrocene prepared via in-situ reaction of *n*-BuLi and ferrocene with the purity of less than 88%,[37,11a] the A_2 monomer of 1,1′-bis(dimethylsilyl)ferrocene prepared by using an excess of *n*-butyllithium and chlorosilanes to ferrocene and combined column chromatography fractionation possesses higher purity. So our approach provides an effective way to synthesize hb-PCS with appreciable molecular weight and regular hyperbranched architecture.

Hyperbranched Ferrocene-Containing Polyborocarbosilanes via Approach 1 (hb-PBCS-BBN). As illustrated in Scheme 1, hb-PBCS-BBN are obtained by the hydroboration of hb-PCS-Vi-precursors and 9-BBN. Since 9-BBN is a monofunctional borane with high regioselectivity widely used in the modification of linear polycarbosilanes,[38] the advantage of this approach is the reservation of hyperbranched architectures and favorable processing properties of hb-PFCS-Vi-precursors.

Figure 8 shows the ^{1}H NMR spectra of hb-PBCS-BBN with different feed ratios of 9-BBN (Table 2). Compared with their hb-PCS-Vi-precursor (Figure 2a), hb-PBCS-BBN shows the

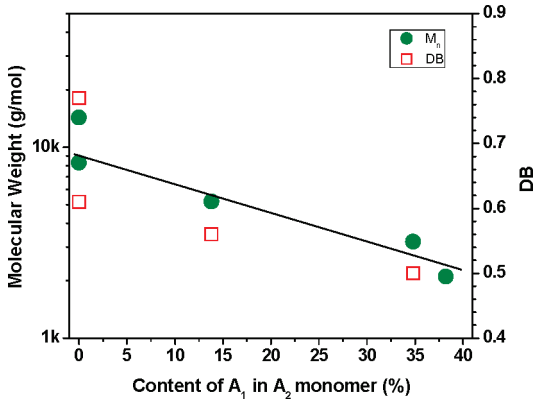

Figure 7. Dependence of molecular weight and DB of hb-PCS-Vi on the content of monosubstituted A_1 in A_2 monomer.

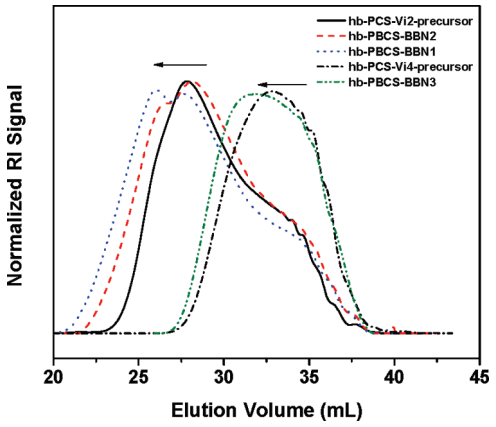

Figure 9. SEC traces (RI signal) of hb-PBCS-BBN from hb-PCS-Vi-precursors.

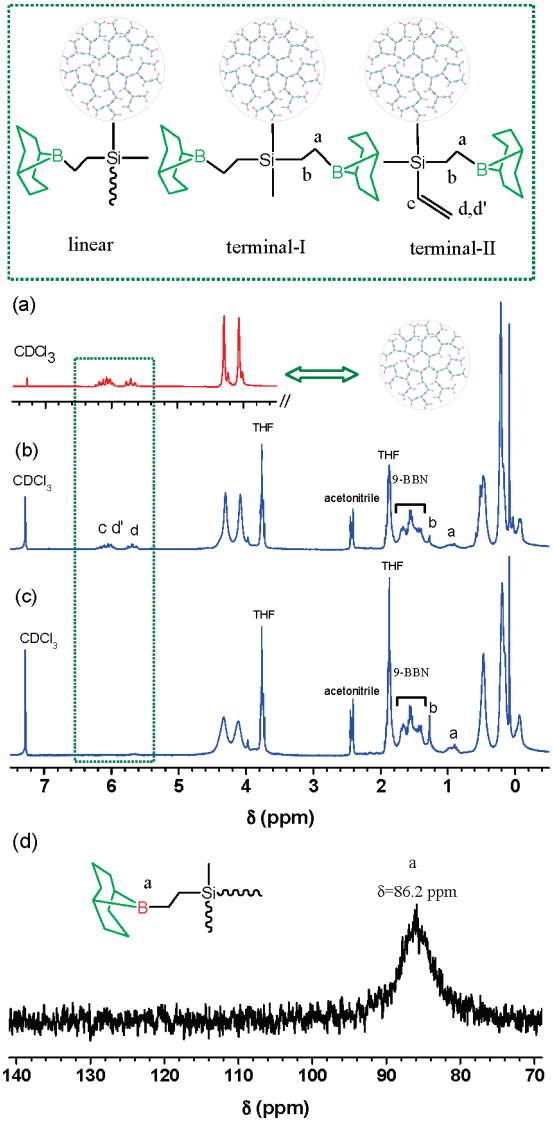

Figure 8. ^{1}H and ^{11}B NMR spectra of hb-PBCS-BBN in $CDCl_3$: (a) ^{1}H NMR of hb-PCS-Vi-precursor, (b) ^{1}H NMR of hb-PBCS-BBN2, (c) ^{1}H NMR of hb-PBCS-BBN1, and (d) ^{11}B NMR of hb-PBCS-BBN1. The inset in (a) is the schematic diagram of hb-PCS-Vi.

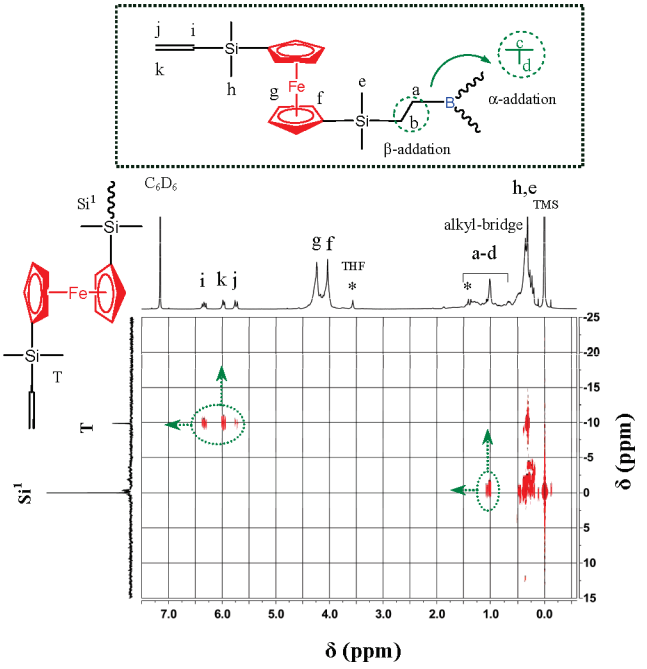

Figure 10. $^{1}H-^{29}Si$ HMBC spectrum of hb-PBCS-Vi in C_6D_6.

decreased integrated areas of vinyl proton resonances (5.82−6.06 ppm) when the Cp ring resonance (4.15 and 4.35 ppm) is employed as an internal standard. At the same time, the appearance of two new signals at 0.9 and 1.24 ppm and a broad peak in the region of 1.36−1.76 ppm correspond to the protons on the resulting methylene (alkyl bridge) and 9-BBN, respectively. The hydroboration occurred mainly via β-addition of 9-BBN with high regioselectivity.[38a] Additionally, the hydroboration is also verified by ^{11}B NMR spectroscopy. The chemical shift of 9-BBN on ^{11}B NMR is at ca. 28 ppm.[38] After the hydroboration, the appearance of new peak at 86.2 ppm in Figure 8d is assignable to boron attached to three ethylene groups. Thus, it clearly indicates the vinyl groups of hb-PFCS-Vi-precursor are added with 9-BBN.

If an excess of 9-BBN was employed, the characteristic signals of vinyl protons of hb-PFCS-Vi-precursor completely disappeared as shown in Figure 8c. For the hb-PBCS-BBN1, it means

Table 3. Macromolecular Conformation Parameters of hb-PBCS from Triple SEC

sample name	dn/dc (mL/g)[a]	$10^{-3}M_{w,triple}$[b]	PDI[b]	$[\eta]_w$ (mL/g)[b]	10^2K (mL/g)[b]	α[b]	g' at $M_{w,triple}$[c]
hb-PCS-Vi1	0.142	282	4.13	18.2	19.4	0.38	0.21
hb-PCS-Vi2	0.156	41.3	3.13	13.8	18.5	0.42	0.62
hb-PCS-SiH1	0.169	152.1	5.17	16.7	26.3	0.36	0.30
hb-PBCS-Vi1	0.120	5.8	1.65	3.8	7.83	0.47	0.70[d]
L-PCS	0.169	5.9	1.26	6.7	1.73	0.69	

[a] The refractive index increment (dn/dc) value of sample in THF was determined on DnDc-2010 (PSS) at 25 °C. [b] The macromolecular structure parameters were determined by triple SEC. [c] g' was calculated from $[\eta]_{hyperbranched}/[\eta]_{linear}$ at M_w, $[\eta]_{hyperbranched} = KM_w^{\alpha}$ (K and α are presented in Table 3), $[\eta]_{linear} = 1.731\times 10^{-2}M_w^{0.692}$. [d] hb-PBCS-Vi1 also uses L-PCS as linear analogue.

almost all the available vinyl groups are added with 9-BBN. By regulating the feed ratio, the content of 9-BBN terminals can be controlled as summarized in Table 2.

The hydroboration efficiency was also demonstrated by the SEC analysis in Figure 9. Compared to hb-PFCS-Vi-precursor, the main peaks of hb-PBCS-BBN on differential refractometer (RI) chromatogram shift to lower elution volume, corresponding to higher hydrodynamic radius and increased molecular weight after hydroboration. From Table 2, the molecular weight increased in correspondence with the increased feed ratio of 9-BBN. Thus, the NMR and SEC results demonstrate that hb-PBCS with boron atoms on termini are successfully synthesized. They are soluble in aliphatic and aromatic solvents but sensitive to air and moisture.

Hyperbranched Ferrocene-Containing Polyborocarbosilanes via Approach 2 (hb-PBCS-Vi). Normally, multifunctional boranes were used as cross-linkers of various linear organometallic polymers such as polysilazanes,[24] polycarbosilanes,[39] and polysilylcarbodiimides.[40] The merit is the higher boron content than 9-BBN. However, the extensive cross-linking always leads to insolubility and poor processability. Here, we present the synthesis of soluble hb-PBCS with boron atoms on the backbone via the "$A_2 + B_3$" route (approach 2) in Scheme 2. Similar to hb-PCS, the starting ratio monomer 4/$BH_3\cdot SMe_2$ of 2:1 (mol/mol) results in hb-PBCS with vinyl terminals (hb-PBCS-Vi). The hb-PBCS-Vi possessing M_w of 3500−5800 are yellow powders and soluble in aliphatic and aromatic hydrocarbons such as THF, 1,4-dioxane, and toluene.

The $^1H-^{29}Si$ HMBC spectrum of hb-PBCS-Vi in C_6D_6 is presented in Figure 10. Compared to the starting monomer 1 (Figure 1c and Figure S1), an obvious decrease of integrated areas ratio of vinyl proton resonances (5.82 and 6.06 ppm) to Cp ring resonances is observed. It is attributed to the hydroboration of vinyl groups with $BH_3\cdot SMe_2$. From the ^{29}Si NMR spectrum, it is clear that there are two types of silicon atoms in the polymer. The first one with $\delta = -0.1$ ppm is correlated with Cp and alkyl bridges and the second one with $\delta = 9.8$ ppm is correlated with Cp and vinyl groups. In another words, the silicon atoms are on backbones and termini in the hyperbranched polymer proposed in Scheme 3. However, because of the high sensitivity of hb-PBCS-Vi, it is not easy to identify the boron atoms that attach to three alkyl groups, i.e., dendritic units. Thus, we will characterize the hyperbranched architecture of hb-PBCS-Vi by their compact conformation in solution.

Intrinsic Viscosity. In order to study the compact conformation of hb-PBCS, their intrinsic viscosity values, $[\eta]$, were measured in THF at 25 °C by triple SEC. The intrinsic viscosity of polymers is related with their molecular weight by the Mark−Houwink−Sakurada (MHS) equation, $[\eta] = KM^{\alpha}$. The MHS exponent, α, is a parameter corresponding to the topology of a polymer in a good solvent. For hyperbranched polymers, the exponent typically varies between 0.5 and 0.2, depending on the degree of branching. In contrast, the MHS exponent is typically in the region of 0.6−0.8 for a linear polymer in a good solvent with a random coil conformation.[41]

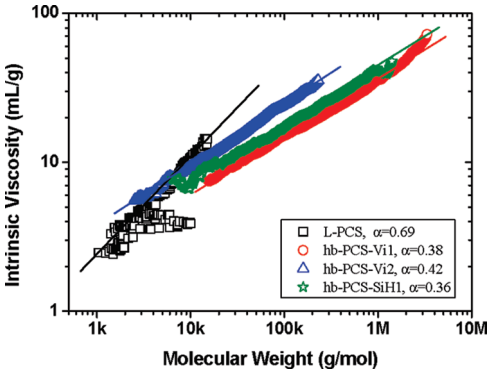

Figure 11. Mark−Houwink−Sakurada plots of L-PCS and hb-PCS.

The triple-SEC results of hb-PBCS are summarized in Table 3, and the MHS plots are presented in Figure 11. As a comparison, the linear analogue (L-PCS) is prepared via the hydrosilylation of monomers **1** and **2**, where ^1H NMR and SEC results are shown in Figures S6 and S7, respectively. The MHS exponent $\alpha = 0.692$ indicates the random coil conformation of L-PCS. In contrast, the MHS exponents of hb-PBCS are significantly lower (α = 0.36−0.47). It evidently demonstrates their hyperbranched architectures and compact shapes in THF solution. With the increase of DB values from 0.54 to 0.79 (Table 1), the α values decreased from 0.42 to 0.36. It indicates that a hyperbranched polymer with higher DB possesses a more compact structure.

The contraction factor, $g' = [\eta]_{hyperbranched}/[\eta]_{linear}$, is another way to express the compact structure of a hyperbranched polymer.[42] According to the results in Table 3, $[\eta]_{linear}$ can be obtained from eq 3

$$[\eta]_{linear} = 1.731 \times 10^{-2}M^{0.692} \quad (3)$$

Experimentally, g' can be expressed as the value at M_w or as a continuous function of molecular weight. Figure 12 shows g' as a function of the molecular weight for representative hyperbranched polymers. The contraction factors decrease with increasing molecular weights and increasing DB, indicating a highly compact structure of hb-PBCS in solution. From the tapping-mode AFM height image and TEM image in Figure S8, it further reveals the particle-like compact shapes with an average dimension of ca. 16 nm for hb-PCS with $M_{w,triple}$ = 282 kg/mol

dx.doi.org/10.1021/ma1029086 |*Macromolecules* 2011, 44, 1280–1291

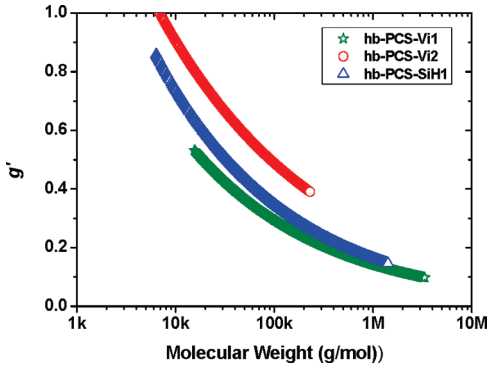

Figure 12. Contraction factors, $g' = [\eta]_{hyperbranched}/[\eta]_{linear}$, for hb-PCSs. The curve of $[\eta]_{hyperbranched}$ vs molecular weight for hb-PCS was obtained from Figure 11. $[\eta]_{linear} = 1.731 \times 10^{-2}M^{0.692}$, where M corresponds to the molecular weight of hb-PCS.

and DB = 0.77. Especially, the value of $g' = 0.70$ at $M_w = 5800$ g/mol of hb-PBCS-Vi1 in Table 3 indicates that hb-PBCS-Vi1 is more compact than the linear analogue. Combined with the α value of 0.47, this suggests the hyperbranched architecture of hb-PBCS-Vi synthesized via approach 2.

CONCLUSIONS

Hyperbranched ferrocene-containing poly(boro)carbosilanes with molecular weights up to 62 300 g/mol (PDI 1.95−4.51) and DB of 0.47−0.79 can be obtained via the hydrosilylation of A_2 monomer, 1,1′-bis(dimethylsilyl)ferrocene and B_3 monomer, trivinylmethylsilane. The molecular weight is conveniently controlled by regulating the polymerization process such as the multibatch addition mode and the usage of high-purity A_2 monomer. Hydroboration of hb-PCS precursor with 9-BBN leads to hb-PBCS with boron atoms on the termini. We believe that the regular hyperbranched architectures favors processability. Additionally, hb-PBCS with boron atoms on the backbone can be generated by the direct hydroboration of 1,1′-bis(dimethylvinylsilyl)ferrocene with the borane−dimethyl sulfide complex. The resulted polymers are soluble in aliphatic and aromatic hydrocarbons with high sensitivity to air and moisture. The combined characterization using NMR and triple SEC demonstrated their hyperbranched architectures.

The tunable and versatile hyperbranched ferrocene-containing poly(boro)carbosilanes promise potential in preparing magnetic and high-temperature-resistant nanostructured ceramics. The pyrolysis mechanism and conversion of hb-PBCS into magnetic and high-temperature-resistant nanostructured ceramics via a direct bulk pyrolysis are currently in progress.

ASSOCIATED CONTENT

Supporting Information. ^{29}Si NMR, MS, and FT-IR results of A_2 monomers; NMR and SEC results of linear poly(ferrocenyl)carbosilane; AFM and TEM images of a hb-PCS. This material is available free of charge via the Internet at http://pubs.acs.org.

AUTHOR INFORMATION

Corresponding Author
*E-mail: axel.mueller@uni-bayreuth.de.

ACKNOWLEDGMENT

Financial support from the National Natural Science Foundation of China (20874080/20604019), the Aoxiang Star Project in Northwestern Polytechnical University, and the Aero-Science Foundation of China (2009ZH53073) is acknowledged. J.K. sincerely thanks the Alexander von Humboldt Foundation for granting a research fellowship. The authors thank Prof. Bernd Wrackmeyer (Inorganic Chemistry II, University of Bayreuth) for the helpful discussion on boron chemistry. The help of Marietta Böhm, Minchang Wang, Peter Thoma, and Zhicheng Zheng for the measurements of triple SEC, ^{29}Si NMR, ^{11}B NMR, and AFM, respectively, is also gratefully acknowledged.

REFERENCES

(1) (a) Colombo, P.; Mera, G.; Riedel, R.; Sorarù, G. D. *J. Am. Ceram. Soc.* **2010**, *93*, 1805–1837. (b) Wideman, T.; Sneddon, L. G. *Chem. Mater.* **1996**, *8*, 3–5. (c) Bernard, S.; Weinmann, M.; Cornu, D.; Miele, P.; Aldinger, F. *J. Eur. Ceram. Soc.* **2005**, *25*, 251–256. (d) Kokott, S.; Heymann, L.; Motz, G. *J. Eur. Ceram. Soc.* **2008**, *28*, 1015–1021.

(2) (a) Wilson, A. M.; Zank, G.; Eguchi, K.; Xing, W.; Yates, B.; Dahn, J. R. *Chem. Mater.* **1997**, *9*, 2139–2144. (b) Iwamoto, Y.; Sato, K.; Kato, T.; Inada, T.; Kubo, Y. *J. Eur. Ceram. Soc.* **2005**, *25*, 257–264. (c) Colombo, P. *J. Eur. Ceram. Soc.* **2008**, *28*, 1389–1395.

(3) (a) Günthner, M.; Kraus, T.; Dierdorf, A.; Decker, D.; Krenkel, W.; Motz, G. *J. Eur. Ceram. Soc.* **2009**, *10*, 2061–2068. (b) Schulz, M. *Adv. Appl. Ceram* **2009**, *108*, 454–460. (c) Liew, L. A.; Zhang, W. G.; An, L. N.; Shah, S.; Luo, R. L.; Liu, Y. P.; Cross, T.; Dunn, M. L.; Bright, V.; Daily, J. W.; Raj, R.; Anseth, K. *Am. Ceram. Soc. Bull.* **2001**, *80*, 25–30. (d) Liew, L. A.; Liu, Y. P.; Luo, R. L.; Cross, T.; An, L. N.; Bright, V. M.; Dunn, M. L.; Daily, J. W.; Raj, R. *Sens. Actuators, A* **2002**, *95*, 120–134.

(4) (a) Riedel, R.; Greiner, A.; Miehe, G.; Dressler, W.; Fuess, H.; Bill, J.; Aldinger, F. *Angew. Chem., Int. Ed.* **1997**, *36*, 603–606. (b) Mera, G.; Riedel, R.; Poli, F.; Müller, K. *J. Eur. Ceram. Soc.* **2009**, *29*, 2873–2883.

(5) (a) Zhang, G. J.; Ohji, T. *J. Am. Ceram. Soc.* **2001**, *84*, 1475–1479. (b) Wideman, T.; Fazen, P. J.; Su, K.; Remsen, E. E.; Zank, G. A.; Sneddon, L. G. *Appl. Organomet. Chem.* **1998**, *12*, 681–693.

(6) (a) Trassl, S.; Suttor, D.; Motz, G.; Rössler, E.; Ziegler, G. *J. Eur. Ceram. Soc.* **2000**, *20*, 215–225. (b) Trassl, S.; Kleebe, H.-J.; Störmer, H.; Motz, G. *J. Am. Ceram. Soc.* **2002**, *85*, 1268–1274.

(7) (a) Baldus, H. P.; Jansen, M.; Wagner, O. *Key Eng. Mater.* **1994**, *75*, 89–91. (b) Weinmann, M.; Haug, R.; Bill, J.; Guire, M.; Aldinger, F. *Appl. Organomet. Chem.* **1998**, *12*, 725–734.

(8) (a) Nguyen, P.; Gómez-Elipe, P.; Manners, I. *Chem. Rev.* **1999**, *99*, 1515–1548. (b) Blackstone, V.; Soto, A. P.; Manners, I. *Dalton Trans.* **2008**, 4363–4371. (c) Abd-El-Aziz, A. S.; Shipman, P. O.; Boden, B. N.; McNeil, W. S. *Prog. Polym. Sci.* **2010**, *35*, 714–836.

(9) (a) Foucher, D. A.; Tang, B. Z.; Manners, I. *J. Am. Chem. Soc.* **1992**, *114*, 6246–6248. (b) Manners, I. *Chem. Commun.* **1999**, 857–865.

(10) (a) Maclachlan, M. J.; Ginzburg, M.; Coombs, N.; Coyle, T. M.; Raju, N. P.; Greedan, J. E.; Ozin, G. A.; Manners, I. *Science* **2000**, *287*, 1460–1463. (b) Nguyen, P.; Gómez-Elipe, P.; Manners, I. *Chem. Rev.* **1999**, *99*, 1515–1548. (c) Kumar, M.; Pannell, K. H. *J. Inorg. Organomet. Polym.* **2008**, *18*, 131–142.

(11) (a) Sun, Q. H.; Lam, J. W. Y.; Xu, K. T.; Xu, H. Y.; Cha, J. A. K.; Wong, P. C. L.; Wen, G. H.; Zhang, X. X.; Jing, X. B.; Wang, F. S.; Tang, B. Z. *Chem. Mater.* **2000**, *12*, 2617–2624. (b) Sun, Q. H.; Xu, K. T.; Peng, H.; Zheng, R. H.; Haussler, M.; Tang, B. Z. *Macromolecules* **2003**, *36*, 2309–2320. (c) Shi, J. B.; Tong, B.; Li, Z.; Shen, J. B.; Zhao, W.; Fu, H. H.; Zhi, J. G.; Dong, Y. P.; Ha1ussler, M.; Lam, J. W. Y.; Tang, B. Z. *Macromolecules* **2007**, *40*, 8195–8204.

(12) Gädt, T.; Ieong, N. S.; Cambridge, G.; Winnik, M. A.; Manners, I. *Nature Mater.* **2009**, *8*, 144–150.

(13) Kulbaba, K.; Cheng, A.; Bartole, A.; Greenberg, S.; Resendes, R.; Coombs, N.; Safa-Sefat, A.; Greedan, J. E.; Stöver, H. D. H.; Ozin, G. A.; Manners, I. *J. Am. Chem. Soc.* **2002**, *124*, 12522–12534.

(14) Wang, X. S.; Guerin, G.; Wang, H.; Wang, Y. S.; Manners, I.; Winnik, M. A. *Science* **2007**, *317*, 644–647.
(15) (a) Rider, D. A.; Liu, K.; Eloi, J. C.; Vanderark, L.; Yang, L.; Wang, J. Y.; Grozea, D.; Lu, Z. H.; Russell, T. P.; Manners, I. *ACS Nano* **2008**, *2*, 263–270. (b) Wurm, F.; Hilf, S.; Frey, H. *Chem.—Eur. J.* **2009**, *15*, 9068–9077.
(16) Riedel, R.; Kienzle, A.; Dressler, W.; Ruwisch, L.; Bill, J.; Aldinger, F. *Nature* **1996**, *382*, 796–798.
(17) (a) Schmidt, W. R.; Narsavage-Heald, D. M.; Jones, D. M.; Marchetti, P. S.; Raker, D.; Maciel, G. E. *Chem. Mater.* **1999**, *11*, 1455–1464. (b) Baldus, H. P.; Jansen, M. *Angew. Chem., Int. Ed.* **1997**, *36*, 328–343. (c) Bill, J.; Aldinger, F. *Adv. Mater.* **1995**, *7*, 775–787. (d) Müller, A.; Gerstela, P.; Butchereit, E.; Nickel, K. G.; Aldinger, F. *J. Eur. Ceram. Soc.* **2004**, *24*, 3409–3417.
(18) (a) Donaghy, K. J.; Carroll, P. J.; Sneddon, L. G. *Inorg. Chem.* **1997**, *36*, 547–553. (b) Boshra, R.; Venkatasubbaiah, K.; Doshi, A.; Jäkle., F. *Organometallics* **2009**, *28*, 4141–4149. (c) Eckensberger, U. D.; Kunz, K.; Bolte, M.; Lerner, H. W.; Wagner, M. *Organometallics* **2008**, *27*, 764–768. (d) Bauer, F.; Braunschweig, H.; Schwab, K. *Organometallics* **2010**, *29*, 934–938.
(19) (a) Scheibitz, M.; Li, H. Y.; Schnorr, J.; Perucha, A. S.; Bolte, M.; Lerner, H. W.; Jäkle, F.; Wagner, M. *J. Am. Chem. Soc.* **2009**, *131*, 16319–16329. (b) Parab, K.; Jäkle, F. *Macromolecules* **2009**, *42*, 4002–4007. (c) Jäkle., F.; Berembaum, A.; Lough, A. J.; Manners, I. *Chem.—Eur. J.* **2000**, *6*, 2762–2771. (d) Heilmann, J. B.; Scheibitz, M.; Qin, Y.; Sundararaman, A.; Jäkle, F.; Kretz, T.; Bolte, M.; Lerner, H. W.; Holthausen, M. C.; Wagner, M. *Angew. Chem.* **2006**, *118*, 934–939.
(20) (a) Kroke, E.; Li, Y. L.; Konetschny, C.; Lecomte, E.; Fasel, C.; Riedel, R. *Mater. Sci. Eng. R* **2000**, *26*, 97–199. (b) Bechelany, M.; Bernard, S.; Brioude, A.; Cornu, D.; Stadelmann, P.; Charcosset, C.; Fiaty, K.; Miele., P. *J. Phys. Chem. C* **2007**, *111*, 13378–13384. (c) Bechelany, M.; Brioude, A.; Stadelmann, P.; Bernard, S.; Cornu, D.; Miele, P. *J. Phys. Chem. C* **2008**, *112*, 18325–18330.
(21) (a) Gutenberger, V. P.; Habel, W.; Nover, C.; Sartori, P. *J. Organomet. Chem.* **1993**, *543*, 1–5. (b) Eber, M.; Jones, L. E. *Ceram. Eng. Sci. Proc.* **1998**, *19*, 485–492. (c) Ngoumeni-Yappi, R.; Fasel, C.; Riedel, R.; Ischenko, V.; Pippel, E.; Woltersdorf, J.; Clade, J. *Chem. Mater.* **2008**, *20*, 3601–3608.
(22) (a) Su, K.; Remsen, E. E.; Zank, G. A.; Sneddon, L. G. *Chem. Mater.* **1993**, *5*, 547–556. (b) Wideman, T.; Su, K.; Remsen, E. E.; Zank, G. A.; Sneddon, L. G. *Chem. Mater.* **1995**, *7*, 2203–2212.
(23) (a) Guron, M. M.; Wei, X. L.; Welna, D.; Krogman, N.; Kim, M. J.; Allcock, H.; Sneddon, L. G. *Chem. Mater.* **2009**, *21*, 1708–1715. (b) Brunner, A. R.; Bujalski, D. R.; Moyer, E. S.; Su, K.; Sneddon, L. G. *Chem. Mater.* **2000**, *12*, 2770–2780. (c) Kong, J.; Fan, X. D.; Si, Q. F.; Zhang, G. B.; Wang, S. J.; Wang, X. *J. Polym. Sci., Part A: Polym. Chem.* **2006**, *44*, 3930–394.
(24) (a) Nghiem, Q. D.; Jeon, J. K.; Hong, L. Y.; Kim, D. P. *J. Organomet. Chem.* **2003**, *688*, 27–35. (b) Jaschke, B.; Klingebiel, U.; Riedel, R.; Doslik, N.; Gadow, R. *Appl. Organomet. Chem.* **2000**, *14*, 671–685.
(25) (a) Emrick, T.; Chang, H. T.; Fréchet, J. M. J. *Macromolecules* **1999**, *32*, 6380–6382. (b) Wang, S. J.; Fan, X. D.; Kong, J.; Lu, J. R. *Polymer* **2009**, *50*, 3587–3594. (c) Wang, S. J.; Fan, X. D.; Kong, J.; Wang, X.; Liu, Y. Y.; Zhang, G. B. *J. Polym. Sci., Part A: Polym. Chem.* **2008**, *46*, 2708–2720. (d) Gao, C.; Yan, D. Y. *Macromolecules* **2001**, *34*, 156–161.
(26) (a) Voit, B. I.; Lederer, A. *Chem. Rev.* **2009**, *109*, 5924–5973. (b) Yates, C. R.; Hayes, W. *Eur. Polym. J.* **2004**, *40*, 1257–1281. (c) Gao, C.; Yan, D. *Prog. Polym. Sci.* **2004**, *29*, 183–275. (d) Jikei, M.; Kakimoto, M. *Prog. Polym. Sci.* **2001**, *26*, 1233–1285. (e) Wurm, F.; Schüle, H.; Frey, H. *Macromolecules* **2008**, *41*, 9602–9611.
(27) Jain, R.; Choi, H.; Lalancette, R. A.; Sheridan, J. B. *Organometallics* **2005**, *24*, 1468–1476.
(28) Rausch, M. D.; Ciappenelli, D. J. *J. Organomet. Chem.* **1967**, *10*, 127–136.
(29) (a) Hölter, D.; Burgath, A.; Frey, H. *Acta Polym.* **1997**, *48*, 30–35. (b) Frey, H.; Hölter, D. *Acta Polym.* **1999**, *50*, 67–76.
(30) Hawker, C. J.; Lee, R.; Fréchet, J. M. J. *J. Am. Chem. Soc.* **1991**, *113*, 4583–4588.
(31) Zhang, G. B.; Kong, J.; Fan, X. D.; Li, X. G.; Tian, W. *Appl. Organomet. Chem.* **2009**, *23*, 277–282.
(32) Schmaljohann, D.; Voit, B. I. *Macromol. Theory Simul.* **2003**, *12*, 679–689.
(33) (a) Malmström, E.; Hult, N. *Macromol. Chem. Phys.* **1997**, *37*, 555–579. (b) Kim, Y. H. *J. Polym. Sci., Polym. Chem. Ed.* **1998**, *36*, 1685–1698. (c) Voit, B. I. *J. Polym. Sci., Part A: Polym. Chem.* **2000**, *38*, 2505–2525.
(34) Grcev, S.; Schoenmakers, P.; Iedema, P. *Polymer* **2004**, *45*, 39–48.
(35) Bharathi, P.; Moore, J. S. *Macromolecules* **2000**, *33*, 3213–3218.
(36) (a) Radke, W.; Litvinenko, G.; Müller, A. H. E. *Macromolecules* **1998**, *31*, 239–248. (b) Mori, H.; Chan Seng, D.; Lechner, H.; Zhang, M. F.; Müller, A. H. E. *Macromolecules* **2002**, *35*, 9270–9281.
(37) Rausch, M. D.; Ciappenelli, D. J. *J. Organomet. Chem.* **1967**, *10*, 127–136.
(38) (a) Lehnert, C.; Trommer, K.; Roewer, G. *Silicon Chem.* **2003**, *2*, 255–264. (b) Puerta, A. R.; Remsen, E. E.; Bradley, M. G.; Sherwood, W.; Sneddon, L. G. *Chem. Mater.* **2003**, *15*, 478–485.
(39) Müller, A.; Gerstel, P.; Weinmann, M.; Bill, J.; Aldinger, F. *Chem. Mater.* **2002**, *14*, 3398–3405.
(40) (a) Weinmann, M.; Haug, R.; Bill, J.; Aldinger, F.; Schuhmacher, J.; Müller, K. *J. Organomet. Chem.* **1997**, *541*, 345–353. (b) Weinmann, M.; Haug, R.; Bill, J.; de Guire, M.; Aldinger, F. *Appl. Organomet. Chem.* **1998**, *12*, 725–734.
(41) Mori, H.; Müller, A. H. E.; Simon, P. F. W. In *Macromolecular Engineering: Precise Synthesis, Materials, Properties, Applications*; Matyjaszewski, K., Gnanou, Y., Leibler, L., Eds.; Wiley-VCH: Weinheim; 2007; Vol. 2, p 973.
(42) Burchard, W. *Adv. Polym. Sci.* **1999**, *143*, 113–194.